

Genomic imprinting of experience-dependent cortical plasticity by the ubiquitin ligase gene *Ube3a*

Masaaki Sato^{a,b,1} and Michael P. Stryker^{a,1}

^aW.M. Keck Foundation Center for Integrative Neuroscience, Department of Physiology, University of California, San Francisco, CA 94143-0444; and ^bLaboratory for Synaptic Function, RIKEN Brain Science Institute, Saitama 351-0198, Japan

Contributed by Michael P Stryker, February 3, 2010 (sent for review November 3, 2009)

A defect in the maternal copy of a ubiquitin ligase gene *Ube3a* can produce a neurodevelopmental defect in human children known as Angelman syndrome. We investigated the role of the maternally expressed *Ube3a* gene in experience-dependent development and plasticity of the mouse visual system. As demonstrated by optical imaging, rapid ocular dominance (OD) plasticity after brief monocular deprivation (MD) was severely impaired during the critical period (CP) in the visual cortex (VC) of *Ube3a* maternal-deficient (m−/p+) mice. Prolonged MD elicited significant plasticity in m−/p+ mice that never matched the level seen in control animals. In older animals after the CP, 7-day MD elicited mild OD shifts in both control and m−/p+ mice; however, the OD shifts in m−/p+ mice lacked the strengthening of visual responses to the two eyes characteristic of normal adult plasticity. Anatomic effects of the maternal deficiency include reduced spine density on basal, but not apical, dendrites of pyramidal neurons in the binocular region of the VC. Imprinting of *Ube3a* expression was not fully established in the early postnatal period, consistent with the normal development of cortical retinotopy and visual acuity that we observed in m−/p+ mice, but was fully established by the onset of the CP. These results demonstrate that paternal and maternal genomes are not functionally equivalent for cortical plasticity, and that maternally expressed *Ube3a* is required for normal experience-dependent modification of cortical circuits during and after the CP.

Angelman syndrome | critical period | epigenetics | ocular dominance plasticity | visual cortex

The majority of autosomal genes in the mammalian genome are expressed from the two alleles that are inherited from the father and mother. But a small subset of genes are silenced in one allele and expressed from the other allele in a parent-of-origin-specific manner. This phenomenon is called genomic imprinting. Intriguingly, many imprinted genes are expressed in the brain (1). Pioneering works using mouse chimaeras have shown that the paternal and maternal genomes are not functionally equivalent in embryogenesis and early brain development (2–5). The role and significance of genomic imprinting in postnatal brain development and experience-dependent plasticity remain to be clarified, however.

The E3 ubiquitin ligase gene *Ube3a* is one of those imprinted genes. *Ube3a* (also known as E6-associated protein; E6AP) is a HECT (homologous to E6-AP carboxyl terminus) domain-containing E3 ubiquitin ligase that was originally identified as the protein mediating human papillomavirus E6-mediated p53 degradation (6). Interestingly, maternal expression of *Ube3a* occurs specifically in the brain in humans and mice (7, 8). The mechanism has been proposed to be parent-of-origin-specific epigenetic modifications of the gene regulatory elements (9, 10). More importantly, genetic abnormalities affecting the imprinting of *Ube3a* in humans are known to cause a neurodevelopmental disorder known as Angelman syndrome (AS) (11, 12), characterized by a range of symptoms including mental retardation, speech impairment, ataxia, seizures with abnormal EEG, and behavioral features, such as frequent laughter (13). Although *Ube3a* maternal-deficient mice have been shown to recapitulate some of the major symptoms of AS in full-grown animals (14), it is important to understand the role of

Ube3a in brain development, given that neurodevelopmental disorders could arise from defects in establishment and refinement of neuronal circuits during the postnatal period (15, 16).

In this study, we sought to elucidate the significance of genomic imprinting in postnatal brain development by taking advantage of the mouse visual system as a model. We report that the maternally expressed *Ube3a* gene plays a key role in experience-dependent cortical plasticity during and after the critical period (CP), a brief developmental time window during which functional connectivity of neural circuits is highly susceptible to altered sensory experience (17). These findings demonstrate a profound impact of parent-specific epigenetic gene regulation on postnatal brain plasticity.

Results

Imprinted Expression of *Ube3a* in Juvenile Mouse Visual Cortex. We examined the expression and localization of *Ube3a* protein in mouse visual cortex (VC) at the peak of the CP for activity-dependent plasticity by immunofluorescent confocal microscopy using anti-*Ube3a* antibodies. Strong *Ube3a* immunoreactivity was observed in neurons in all layers of wild-type (m+/p+) and *Ube3a* paternal-deficient (m+/p−) mice, but not in *Ube3a* maternal-deficient (m−/p+) mice (Fig. 1*A* and Fig. S1*A*). The labeling was localized primarily to the nucleus of both CaMKII-positive excitatory pyramidal neurons and GAD67-positive inhibitory interneurons at this stage of development in this brain region, and nearly all cells were *Ube3a*-positive (Fig. 1*B* and *C*). *Ube3a* immunoreactivity was found in the parvalbumin-positive subpopulation of GABAergic interneurons as well (Fig. S1*B*). *Ube3a* immunoreactivity was found in neurons in the dorsal lateral geniculate nucleus (dLGN) of the thalamus (Fig. S1*B*). Immunoblot analysis confirmed the maternal expression of *Ube3a* in the cortex. *Ube3a* protein levels were similar in m+/p− mice and m+/p+ mice, whereas the *Ube3a* protein levels in m−/p+ mice were indistinguishable from the background levels seen in *Ube3a* homozygous mutant (m−/p−) mice (Fig. 1*D*, *i*). Outside the VC, *Ube3a* protein levels in the prefrontal cortex of m−/p+ mice were virtually undetectable (Fig. 1*D*, *ii*), demonstrating maternal expression of *Ube3a* in other cortical areas. Collectively, these results indicate that by 4 weeks of age, *Ube3a* is expressed almost exclusively from the maternal allele in mouse VC.

Lack of Rapid and Mature Ocular Dominance Plasticity in *Ube3a* Maternal-Deficient VC. We next investigated the ocular dominance (OD) plasticity of the VC in m−/p+ mice during the CP using optical imaging of the intrinsic signal as a measure of visual cortical activity elicited by visual stimulation through the two eyes. This technique relies on a localized change in the reflectance of 610-nm light, which reflects the conversion of oxyhemoglobin to deoxy-

Author contributions: M.S. and M.P.S. designed research; M.S. performed research; M.S. and M.P.S. analyzed data; and M.S. and M.P.S. wrote the paper.

The authors declare no conflict of interest.

¹To whom correspondence may be addressed. E-mail: msato@brain.riken.jp or stryker@phy.ucsf.edu.

This article contains supporting information online at www.pnas.org/cgi/content/full/1001281107/DCSupplemental.

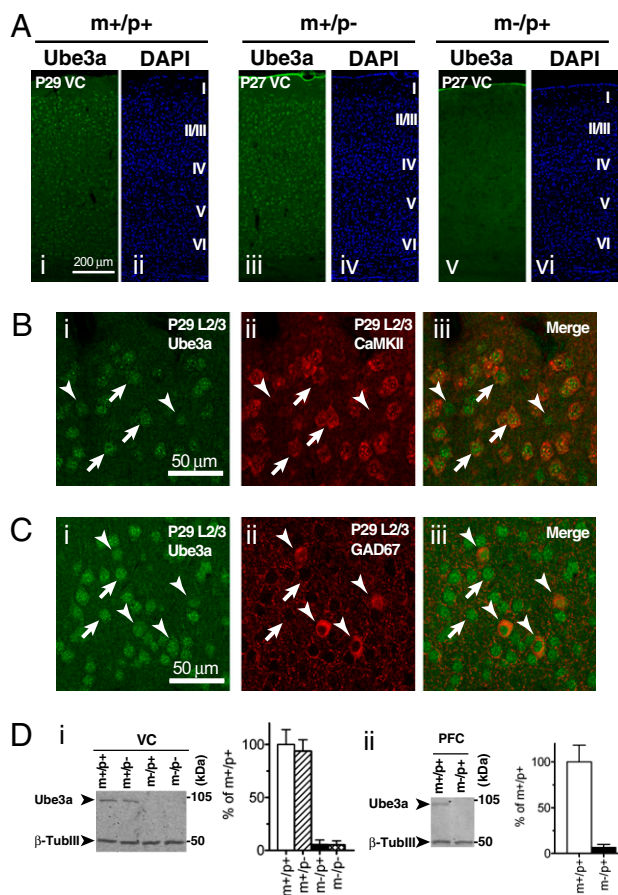


Fig. 1. Imprinting and localization of Ube3a protein in juvenile mouse VC. (A) Imprinted expression of Ube3a in juvenile mouse VC. Confocal images of Ube3a immunofluorescence (*i*, *iii*, and *v*) and DAPI nuclear staining (*ii*, *iv*, and *vi*) in VC of wild-type ($m+/p+$), paternal-deficient ($m+/p-$) and maternal-deficient ($m-/p+$) mice at P27–29. Cortical layers are indicated in Roman numerals on the right of the DAPI images. (Scale bar: 200 μm .) (B) Expression of Ube3a in excitatory neurons. Arrows and arrowheads show Ube3a immunoreactivity in a few representative CaMKII-positive principal neurons and CaMKII-negative neurons, respectively. (Scale bar: 50 μm .) (C) Expression of Ube3a in inhibitory neurons. Arrows and arrowheads indicate Ube3a immunoreactivity in GAD67-negative neurons and GAD67-positive neurons, respectively. (Scale bar: 50 μm .) (D) Immunoblot analysis of Ube3a protein in VC (*i*) and prefrontal cortex (PFC; *ii*). Molecular sizes of marker proteins are indicated on the right. β -tubulin III (β -TubIII) was used as a loading control. Bar graphs show quantification of the Ube3a protein levels expressed as a percentage of those in $m+/p+$ mice ($n = 3$).

hemoglobin by the increased metabolic demand of activated neurons; it correlates well with other measures of neural activity (18). The relative strength of the two eyes in driving cortical cells is measured by an OD index that has positive values for responses favoring the contralateral eye. To measure plasticity, visual responses to the two eyes in binocular VC were imaged before and after a brief period (generally 4 days) of monocular visual deprivation (MD). Our initial nonsurvival experiments revealed that $m+/p+$ and $m+/p-$ mice showed substantial shifts in response toward the nondeprived eye after a 4-day MD (OD index in $m+/p+$ without MD, 0.24 ± 0.02 , $n = 5$; with MD, -0.02 ± 0.03 , $n = 4$; $P < 0.05$ vs. $m+/p+$ without MD; OD index in $m+/p-$ without MD, 0.22 ± 0.01 , $n = 4$; with MD, 0.01 ± 0.03 , $n = 4$; $P < 0.05$ vs. $m+/p-$ without MD), whereas plasticity in $m-/p+$ mice was significantly reduced after similar MD. The OD index after brief MD was significantly higher in $m-/p+$ mice compared with $m+/p+$ and $m+/p-$ mice ($m-/p+$ without MD, 0.18 ± 0.03 , $n = 4$; $m-/p+$ with MD,

0.12 ± 0.01 , $n = 4$; $P < 0.05$ vs. $m+/p+$ or $m+/p-$ with MD) (Fig. S2 A and C). These findings using optical imaging to measure the early phase of plasticity are consistent with those obtained using visual evoked potentials by Yashiro et al. (19), who also found changes in plasticity in vitro. Maximum response magnitude was comparable between $m+/p\pm$ (i.e., $m+/p+$ and $m+/p-$) and $m-/p+$ mice without MD; however, brief MD greatly decreased cortical responsiveness to the deprived contralateral eye in $m+/p\pm$ mice ($m+/p\pm$ without MD, 2.24 ± 0.25 , $n = 9$; $m+/p\pm$ with MD, 1.59 ± 0.13 , $n = 8$; $P < 0.05$), whereas the decrease in $m-/p+$ mice after brief MD was only slight ($m-/p+$ without MD, 2.26 ± 0.23 , $n = 4$; $m-/p+$ with MD, 1.97 ± 0.21 , $n = 4$, $P = 0.34$), suggesting that the lack of robust OD shifts after MD in $m-/p+$ mice was due to a failure of the loss of responsiveness to the deprived eye (Fig. S2 B and C).

Longitudinal studies of OD plasticity by chronic, repeated imaging confirmed and extended these initial findings (Fig. 2 A and B). The effect of 4d MD was much smaller in $m-/p+$ mice ($m+/p+$, $n = 6$; $m-/p+$, $n = 9$; $P < 0.01$); however, more prolonged MD (7–14d) in $m-/p+$ mice eventually elicited an OD shift that was almost as great as that after only 4d MD in $m+/p+$ mice, but much smaller than that after a comparable period of MD ($m+/p+$ after 7d MD, -0.08 ± 0.04 , $n = 6$; $m-/p+$ after 7d MD, 0.06 ± 0.02 , $n = 5$; $P < 0.01$ vs. $m+/p+$ after 7d MD; $m+/p+$ after 14d MD, -0.15 ± 0.01 , $n = 2$; $m-/p+$ after 14d MD, 0.02 ± 0.02 , $n = 6$; $P < 0.01$ vs. $m+/p+$ after 7d and 14d MD). These results demonstrate that Ube3a protein is required at the peak of the CP for rapid, saturating plasticity in VC.

We next studied whether loss of Ube3a impairs adult OD plasticity in mature VC. In $m+/p+$ mice, 7d MD elicited significant OD shifts, but 4d MD did not (pre-MD, 0.22 ± 0.02 ; 4d MD, 0.14 ± 0.02 ; 7d MD, 0.06 ± 0.02 , $n = 5$; $P < 0.01$ pre-MD vs. 7d MD) (Fig. 2 C). The maximum response magnitude to the contralateral deprived eye decreased slightly at 4d MD but returned to the initial strength at 7d MD (contra at pre-MD, 1.54 ± 0.13 ; at 4d MD, 1.37 ± 0.12 ; at 7d MD, 1.46 ± 0.13 , $n = 5$), whereas that to the ipsilateral nondeprived eye remained unchanged at 4d MD but was substantially strengthened at 7d MD (ipsi at pre-MD, 1.06 ± 0.06 ; at 4d MD, 1.07 ± 0.12 ; at 7d MD, 1.35 ± 0.14 , $n = 5$) (Fig. 2 D and F). These data imply that basic features of adult OD plasticity are already evident in the sixth week of life (20). The changes in OD elicited by 4d and 7d MD in post-CP $m-/p+$ mice were similar to those in $m+/p+$ mice (pre-MD, 0.20 ± 0.02 ; at 4d MD, 0.16 ± 0.02 ; at 7d MD, 0.07 ± 0.03 ; $P < 0.01$, pre-MD vs. 7d MD, $n = 7$) (Fig. 2 C); however, $m-/p+$ mice failed to show the normal strengthening of responses to the two eyes after 7d MD. Maximum response magnitude for the contralateral deprived eye continued to decrease further until 7d MD (pre-MD, 1.48 ± 0.12 ; at 4d MD, 1.23 ± 0.08 ; at 7d MD, 0.85 ± 0.08 ; $P < 0.01$ vs. $m+/p+$ at 7d MD, $n = 7$), whereas that for the ipsilateral nondeprived eye lacked potentiation of the response (pre-MD, 1.00 ± 0.05 ; at 4d MD, 0.94 ± 0.06 ; at 7d MD, 0.82 ± 0.07 ; $P < 0.01$ vs. $m+/p+$ at 7d MD, $n = 7$) (Fig. 2 D and F). These results suggest that the OD plasticity in $m-/p+$ mice in post-CP differs qualitatively from that in $m+/p+$ mice, lacking the substantial strengthening of the visual responses to the two eyes normally seen after prolonged MD in mature VC.

The reduced rapid OD plasticity in $m-/p+$ mice at P25–28 could result from a change in cortical maturation that alters the timing of the CP. An analysis of net OD shifts after 4d MD at P21–22 and P33–37 (before and after the normal peak of the CP) excluded this possibility (Fig. 2 E). The OD shifts in the CP were significantly smaller in $m-/p+$ mice than in $m+/p+$ mice of the corresponding age ($m+/p+$ in CP, 0.21 ± 0.02 , $n = 6$; $m-/p+$ in CP, 0.06 ± 0.02 , $n = 9$; $P < 0.01$). In $m-/p+$ mice, MD before and after the normal CP elicited smaller changes than those during CP, although not significantly so [post-CP (P33–37) shift, 0.04 ± 0.02 , $n = 7$, $P = 0.68$ vs. $m-/p+$ in CP; pre-CP (P21–22) shift, 0.03 ± 0.01 , $n = 4$; $P = 0.94$ vs. $m-/p+$ in CP]. These results indicate that the loss of Ube3a protein does not delay or advance the peak of CP.

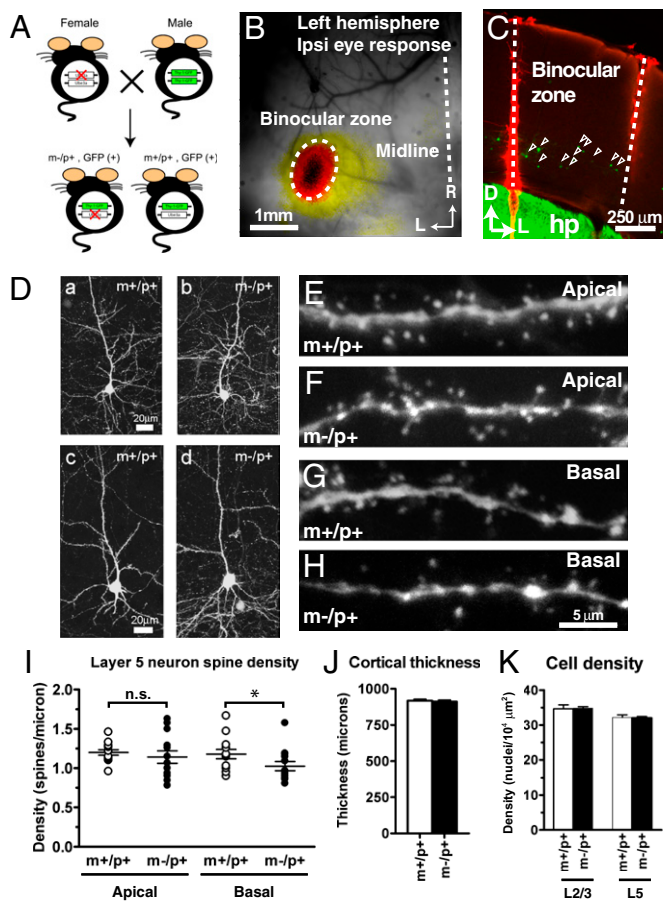


Fig. 3. Subcellular domain-specific reduction of spine density in layer 5 pyramidal neurons in binocular cortex of *m*-/*p*+ mice. (A) *m*-/*p*+ mice bearing GFP-labeled infragranular cortical neurons were genetically obtained from the offspring of female *Ube3a* heterozygotes crossed with male homozygous *thy1-GFP* transgenic mice. (B) Locating binocular VC by optical imaging. Visual response was evoked through the ipsilateral eye by a noise movie presented in binocular visual field. The image of cortical activity was superimposed onto a vasculature image taken under green illumination, R, rostral; L, lateral. (Scale bar: 1 mm.) (C) GFP-labeled infragranular pyramidal neurons (open arrowheads) in binocular zone of the *m*-/*p*+ mouse shown in B. Boundaries of the binocular cortex are designated by red tracks of Dil. hp, hippocampus; D, dorsal; L, lateral. (Scale bar: 250 μ m.) (D) Examples of GFP-labeled layer 5 pyramidal neurons in binocular VC of *m*+/*p*+ (a and c) and *m*-/*p*+ (b and d) mice. (Scale bar: 20 μ m.) (E and F) Maximum intensity projections (MIPs) of secondary apical dendrites of layer 5 pyramidal neurons in *m*+/*p*+ (E) and *m*-/*p*+ (F) binocular VC. (G and H) MIPs of basal dendrites of layer 5 pyramidal neurons in *m*+/*p*+ (G) and *m*-/*p*+ (H) binocular VC. (Scale bar: 5 μ m.) (I) Quantitative analysis of spine density showing that layer 5 pyramidal neurons in *m*-/*p*+ mice have significantly reduced spine density in basal dendrites, but not in apical dendrites ($n = 13$ each; * $P < 0.05$; ns, not significant). (J) Thickness of binocular VC in *m*+/*p*+ (white bar, $n = 3$) and *m*-/*p*+ mice (black bar, $n = 3$). (K) Overall cell density in lower layer 2/3 and layer 5 of binocular VC in *m*+/*p*+ (white bars, $n = 3$) and *m*-/*p*+ mice (black bars, $n = 3$).

in *m*-/*p*+ neurons (*m*+/*p*+, 1.199 ± 0.035 , $n = 13$; *m*-/*p*+, 1.142 ± 0.080 , $n = 13$; $P = 0.34$), but slightly (albeit significantly) reduced density of basal dendrites (*m*+/*p*+, 1.179 ± 0.060 , $n = 13$; *m*-/*p*+, 1.026 ± 0.058 , $n = 13$; $P < 0.05$) (Fig. 3 E–I). Binocular cortex thickness and cell density in lower layer 2/3 and layer 5 did not differ between *m*+/*p*+ and *m*-/*p*+ mice (Fig. 3 J and K), suggesting that *Ube3a* is involved in a cellular process regulating the number of synapses rather than the number of cells. These results collectively indicate that maternal loss of *Ube3a* can reduce spine density in a subcellular domain-specific manner in cortical neurons.

Developmental Regulation of *Ube3a* Imprinting in Mouse VC. Because many molecules involved in neural plasticity are dynamically regulated during development and by visual experience, we investigated whether *Ube3a* protein levels in VC are dynamic as well. As a control, we measured expression levels of the activity-regulated gene product *zif268*. Levels of *Ube3a* appeared to remain quite stable from before eye opening to adulthood, whereas levels of *zif268* increased drastically at P18 after eye opening (Fig. S7 A and B). In addition, 4d MD during the CP sharply reduced the protein levels of *zif268*, but not those of *Ube3a*, in the VC contralateral to the deprived eye (Fig. S7 C and D). These results indicate that *Ube3a* protein levels remain relatively constant during development and insensitive to changes in visual activity.

Immunofluorescence microscopy of *Ube3a* protein revealed incomplete genomic imprinting in the VC during early postnatal development. As in older mice, strong *Ube3a* immunoreactivity was observed in cortical neurons of *m*+/*p*+ mice at P6 (compare Fig. 14, *i* and Fig. 44, *i*). However, unlike in older animals, neurons in *m*-/*p*+ mice at P6 were weakly labeled as well (Fig. 44, *iii*). Control experiments performed in parallel without the primary antibody did not produce the same labeling pattern (Fig. 44, *v*), suggesting that the *Ube3a* signal is specific. Immunoblot analysis of *Ube3a* protein on P6 visual cortical homogenates also supported this observation

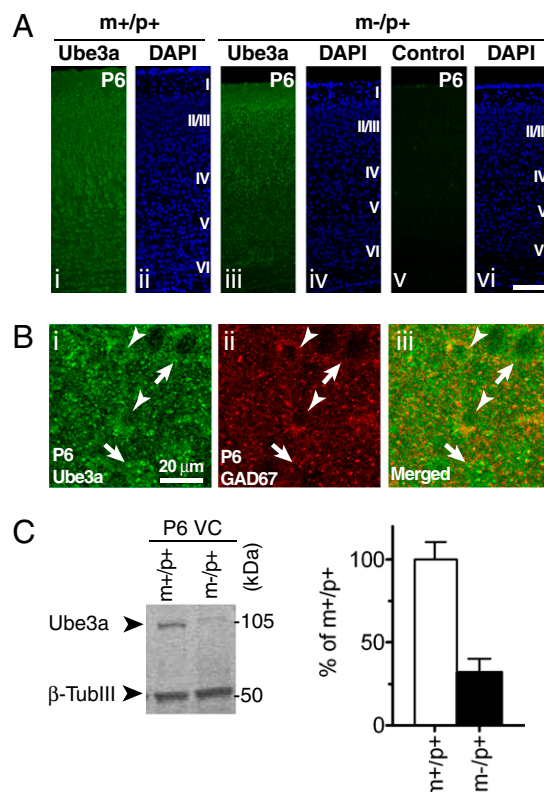


Fig. 4. Relaxed imprinting of *Ube3a* expression in early postnatal VC in mice. (A) Confocal images of *Ube3a* immunofluorescence (*i* and *iii*), control fluorescence without primary antibody against *Ube3a* (*v*), and DAPI nuclear staining (*ii*, *iv*, and *vi*) in VC of *m*+/*p*+ (*i* and *ii*) and *m*-/*p*+ mice (*iii*–*vi*) at P6. Neurons in *m*-/*p*+ mice exhibit weak, but specific, labeling for *Ube3a*. Cortical layers are indicated by Roman numerals on the right of the DAPI images. (Scale bar: 100 μ m.) (B) Expression of *Ube3a* protein in inhibitory neurons during the early postnatal period. *Ube3a* immunoreactivity in GAD67-positive and GAD67-negative neurons is indicated by arrowheads and arrows, respectively. (Scale bar: 20 μ m.) (C) Immunoblot analysis of *Ube3a* protein expression, as shown in Fig. 1D, in VC of *m*+/*p*+ and *m*-/*p*+ mice at P6. Quantification of *Ube3a* levels in VC of *m*-/*p*+ mice at P6 is shown on the right ($n = 4$).

(Fig. 4C). The level of Ube3a protein in m^{-}/p^{+} mice was significantly higher at P6 than at P27–29 (P6, $32\% \pm 8\%$ of m^{+}/p^{+} , $n = 4$; $P < 0.05$ vs. P27–29, m^{-}/p^{+} , $6 \pm 4\%$ of m^{+}/p^{+} ; unpaired *t* test; Figs. 1D, *i* and 4C), indicating that the paternal allele is not completely silenced at this stage.

Subcellular localization of Ube3a also changed during development. In P6 VC, both GAD67-positive and GAD67-negative neurons showed Ube3a immunoreactivity (Fig. 4B). However, unlike in older animals, in which Ube3a expression appeared to be confined largely to the nucleus (Fig. 1B and C), Ube3a immunoreactivity at P6 in m^{+}/p^{+} mice was observed primarily in the cytosol and was similar or lower in the nucleus, and was definitely lower in the nucleus than in the cytosol in m^{-}/p^{+} animals (Fig. 4A and B and Fig. S8A and C).

Discussion

The findings of this study are summarized in Fig. 5. The mouse visual system develops postnatally as a sequence of events including retinotopic map development, eye opening, visual acuity development, opening of the CP for monocular deprivation, and circuit consolidation after the CP. Although expression levels of Ube3a protein in VC are quite stable from the early postnatal period to adulthood, the mode of expression and localization of the protein undergoes dramatic changes. In early postnatal cortex, Ube3a is expressed biallelically, and the protein is present in the cytoplasm of both excitatory and inhibitory neurons. By the time of CP, however, maternal expression of Ube3a is established, and the protein is localized to the nucleus of both excitatory and inhibitory neurons. The Ube3a protein level is not altered by visual deprivation during this period. Similarly, in early postnatal visual development of m^{-}/p^{+} mice, cortical retinotopic maps form normally, the eyes open at the proper time, and visual acuity develops rapidly to normal near-adult levels. Later in development, when imprinting is fully established during the CP, m^{-}/p^{+} mice exhibit impaired rapid experience-dependent plasticity after brief MD. Finally, after the CP, m^{-}/p^{+} mice exhibit plasticity that differs qualitatively from that in m^{+}/p^{+} mice, lacking strengthening of responses for both eyes after prolonged MD. These results imply that imprinting of Ube3a expression exerts a profound influence on circuit development after the early stage of expression.

The lack of rapid OD plasticity after brief MD and marked OD shifts after prolonged MD in the CP closely resemble the plasticity phenotype of GAD65 knockout and CaMKII α phosphorylation-deficient mice (27, 28), although the VC of m^{-}/p^{+} mice exhibits normal levels of GAD expression and CaMKII α phosphorylation (unlike in hippocampus; see also ref. 29). Because the rapid

component of OD plasticity is known to be cortical in origin (26, 30), it is tempting to speculate that the residual component that is preserved in these mutant mice is mediated by a different mechanism, perhaps by slow rearrangement of thalamocortical axons (31, 32), although we have no direct evidence for this.

In contrast to the severe plasticity defects during the CP, plasticity after the CP is less severely affected in m^{-}/p^{+} mice. MD in m^{-}/p^{+} mice produced small OD shifts after the CP that were normal in magnitude but different in character from those in m^{+}/p^{+} mice (20, 33). The lack of strengthening of visual responses after post-CP MD agrees well with the idea that m^{-}/p^{+} mice have defects in maturation and consolidation of cortical circuits after the closure of CP, consistent with recently reported *in vitro* findings (see fig. 5 in ref. 19). Because imprinting of Ube3a also occurs in prefrontal cortex (Fig. 1D, *ii*), the abnormalities in CP and post-CP plasticity may illuminate the severe learning difficulties observed in individuals with AS (13).

Our findings that imprinting and subcellular localization of Ube3a are developmentally regulated are consistent with accumulating evidence that genomic imprinting in the brain can be developmental stage-specific (1). Whether similar changes in expression and subcellular localization take place in the human brain remains unclear (34, 35). Elucidating the mechanism underlying this developmental regulation (if it occurs in humans) may have clinical potential for developing a cure for AS. Effective interventions to keep the paternal allele active later in life could act to compensate for the genetic abnormalities affecting the maternal expression of Ube3a.

Methods

Mice, Surgery, and Intrinsic Signal Optical Imaging. Mice bearing a null mutation for Ube3a were generated and backcrossed onto a C57BL/6 inbred genetic background as described previously (14). All surgical procedures were approved by the University of California San Francisco's Institutional Animal Care and Use Committee. Monocular deprivation, acute optical imaging of OD plasticity, and subsequent data analysis were conducted as described previously (20). Retinotopic maps in VC were imaged as described in *SI Methods*. In chronic experiments, mice were imaged transcranially under anesthesia produced by 0.8% isoflurane following preanesthetic administration of chlorprothixene (1–2 mg/kg *i.p.*). The scalp was sutured at the end of each imaging session. A contrast-modulated stochastic noise movie (spatial frequency cut-off, 0.05 cycle/degree; temporal frequency cutoff, 4 Hz; period, 10 s; duration, 4 min) was used to measure visual responsiveness for each eye (36).

Immunofluorescence. Mice were deeply anesthetized with Nembutal and perfused transcardially with PBS, followed by 4% paraformaldehyde in PBS. Brains were removed and further fixed in 4% PFA and cryoprotected in 30% sucrose in PBS at 4 °C overnight. Frozen sections were cut coronally on a cryostat to a thickness of 30 μ m for juvenile brains and 50 μ m for postnatal brains. Sections were incubated with primary antibodies diluted in PBS containing 2% normal goat serum (Sigma-Aldrich), 0.1% Triton X-100, and 0.05% Na₂S₂O₈ at 4 °C overnight, followed by secondary antibodies diluted in the same buffer for 1 h at room temperature. For nuclear staining, DAPI (0.1 μ g/mL; Sigma-Aldrich) was included in the secondary antibody solution. The primary and secondary antibodies used in the study are listed in *SI Methods*. Images were acquired with a Leica TCS SP5 laser-scanning confocal microscope.

Analysis of Dendritic Spine Density. m^{-}/p^{+} mice bearing GFP-labeled infragranular pyramidal neurons were obtained from the offspring of female Ube3a heterozygous mice crossed with male homozygous GFP-M transgenic mice expressing EGFP under thy1 promoter (25). Before perfusion, the binocular cortex was located by optical imaging, and its boundary was marked using a Dil-coated sharp tungsten microelectrode. Brains were removed, postfixed, and cut coronally into 100- μ m-thick serial sections with a vibratome (Lancer). Cell nuclei were stained with DAPI before mounting. Shrinkage of tissues caused by fixation was not corrected in our quantitative analyses.

Determination of dendritic spine density was performed essentially as described previously (30). With the aid of the Dil tracks and DAPI staining, well-isolated secondary branches of the apical dendrites or basal dendrites of GFP-labeled layer 5 neurons were carefully selected in binocular VC for imaging. High magnification images of the dendrites were acquired with a Leica confocal microscope with a water-immersion 40 \times objective and 4 \times digital zoom. For each

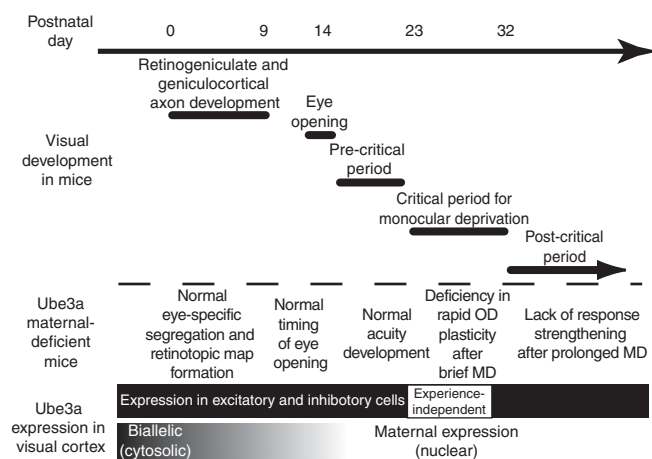


Fig. 5. Imprinting of Ube3a and its role in mouse visual development. (See Discussion for details.)

animal, four or five neurons were imaged at different anteroposterior levels, and a $\geq 30\text{-}\mu\text{m}$ segment of those dendrites was used for quantification. A stack of images spanning the entire depth of the selected dendritic segments was collected at $0.5\text{-}\mu\text{m}$ z-axis intervals. Maximum intensity projection (MIP) of an image stack was created with the Leica LAS AF software. Spines protruding from the dendritic shafts were identified using Leica LAS AF software by examining the serial optical sections one by one, as well as referring to the MIP. Cell density and cortical thickness were measured as described in *SI Methods*.

Retinogeniculate Labeling. Eye-specific segregation of retinogeniculate axons was labeled and imaged in juvenile mice as described in *SI Methods*.

Immunoblot Analysis. Immunoblot analysis of mouse visual cortical homogenates was performed as described in *SI Methods*.

Behavioral Testing of Visual Acuity Development. Visual acuity of unrestrained, freely moving mice was quantified as described in *SI Methods*.

Statistics. All data are expressed as mean \pm SEM. Statistical significance between groups was calculated using the nonparametric Mann-Whitney test unless noted otherwise.

ACKNOWLEDGMENTS. We are grateful to Professor Arthur Beaudet for providing the *Ube3a*-deficient mice and Maha Abdulla for assisting with the behavioral experiments. We also thank Professors Matthew LaVail, Arturo Alvarez-Buylla, and Nigel Bunnnett for sharing their equipment. This work was supported by grants from the National Institutes of Health (EY02874 and MH077972) and the Angelman Syndrome Foundation (to M.P.S.). M.S. is a recipient of fellowships from the Uehara Memorial Foundation and the Japan Society for the Promotion of Science.

1. Wilkinson LS, Davies W, Isles AR (2007) Genomic imprinting effects on brain development and function. *Nat Rev Neurosci* 8:832–843.
2. McGrath J, Solter D (1984) Completion of mouse embryogenesis requires both the maternal and paternal genomes. *Cell* 37:179–183.
3. Barton SC, Surani MA, Norris ML (1984) Role of paternal and maternal genomes in mouse development. *Nature* 311:374–376.
4. Allen ND, et al. (1995) Distribution of parthenogenetic cells in the mouse brain and their influence on brain development and behavior. *Proc Natl Acad Sci USA* 92:10782–10786.
5. Keverne EB, Fundele R, Narasimha M, Barton SC, Surani MA (1996) Genomic imprinting and the differential roles of parental genomes in brain development. *Brain Res Dev Brain Res* 92:91–100.
6. Hübregtse JM, Scheffner M, Howley PM (1993) Cloning and expression of the cDNA for E6-AP, a protein that mediates the interaction of the human papillomavirus E6 oncoprotein with p53. *Mol Cell Biol* 13:775–784.
7. Albrecht U, et al. (1997) Imprinted expression of the murine Angelman syndrome gene, *Ube3a*, in hippocampal and Purkinje neurons. *Nat Genet* 17:75–78.
8. Rougeulle C, Glatt H, Lalonde M (1997) The Angelman syndrome candidate gene, *UBE3A/E6-AP*, is imprinted in brain. *Nat Genet* 17:14–15.
9. Perk J, et al. (2002) The imprinting mechanism of the Prader-Willi/Angelman regional control center. *EMBO J* 21:5807–5814.
10. Horsthemke B, Wagstaff J (2008) Mechanisms of imprinting of the Prader-Willi/Angelman region. *Am J Med Genet A* 146A:2041–2052.
11. Matsuura T, et al. (1997) De novo truncating mutations in E6-AP ubiquitin-protein ligase gene (*UBE3A*) in Angelman syndrome. *Nat Genet* 15:74–77.
12. Kishino T, Lalonde M, Wagstaff J (1997) *UBE3A/E6-AP* mutations cause Angelman syndrome. *Nat Genet* 15:70–73.
13. Clayton-Smith J, Laan L (2003) Angelman syndrome: A review of the clinical and genetic aspects. *J Med Genet* 40:87–95.
14. Jiang YH, et al. (1998) Mutation of the Angelman ubiquitin ligase in mice causes increased cytoplasmic p53 and deficits of contextual learning and long-term potentiation. *Neuron* 21:799–811.
15. Zoghbi HY (2003) Postnatal neurodevelopmental disorders: Meeting at the synapse? *Science* 302:826–830.
16. Ehninger D, Li W, Fox K, Stryker MP, Silva AJ (2008) Reversing neurodevelopmental disorders in adults. *Neuron* 60:950–960.
17. Hubel DH, Wiesel TN (1970) The period of susceptibility to the physiological effects of unilateral eye closure in kittens. *J Physiol* 206:419–436.
18. Kalatsky VA, Stryker MP (2003) New paradigm for optical imaging: Temporally encoded maps of intrinsic signal. *Neuron* 38:529–545.
19. Yashiro K, et al. (2009) *Ube3a* is required for experience-dependent maturation of the neocortex. *Nat Neurosci* 12:777–783.
20. Sato M, Stryker MP (2008) Distinctive features of adult ocular dominance plasticity. *J Neurosci* 28:10278–10286.
21. Hensch TK, et al. (1998) Local GABA circuit control of experience-dependent plasticity in developing visual cortex. *Science* 282:1504–1508.
22. Taha S, Hanover JL, Silva AJ, Stryker MP (2002) Autophosphorylation of alphaCaMKII is required for ocular dominance plasticity. *Neuron* 36:483–491.
23. Cang J, et al. (2005) Development of precise maps in visual cortex requires patterned spontaneous activity in the retina. *Neuron* 48:797–809.
24. Godement P, Salaün J, Imbert M (1984) Prenatal and postnatal development of retinogeniculate and retinocollicular projections in the mouse. *J Comp Neurol* 230:552–575.
25. Feng G, et al. (2000) Imaging neuronal subsets in transgenic mice expressing multiple spectral variants of GFP. *Neuron* 28:41–51.
26. Trachtenberg JT, Trepel C, Stryker MP (2000) Rapid extragranular plasticity in the absence of thalamocortical plasticity in the developing primary visual cortex. *Science* 287:2029–2032.
27. Taha SA, Stryker MP (2005) Ocular dominance plasticity is stably maintained in the absence of alpha calcium calmodulin kinase II (alphaCaMKII) autophosphorylation. *Proc Natl Acad Sci USA* 102:16438–16442.
28. Fagioli M, Hensch TK (2000) Inhibitory threshold for critical-period activation in primary visual cortex. *Nature* 404:183–186.
29. Weeber EJ, et al. (2003) Derangements of hippocampal calcium/calmodulin-dependent protein kinase II in a mouse model for Angelman mental retardation syndrome. *J Neurosci* 23:2634–2644.
30. Taha S, Stryker MP (2002) Rapid ocular dominance plasticity requires cortical but not geniculate protein synthesis. *Neuron* 34:425–436.
31. Antonini A, Stryker MP (1993) Rapid remodeling of axonal arbors in the visual cortex. *Science* 260:1819–1821.
32. Antonini A, Fagioli M, Stryker MP (1999) Anatomical correlates of functional plasticity in mouse visual cortex. *J Neurosci* 19:4388–4406.
33. McGee AW, Yang Y, Fischer QS, Daw NW, Strittmatter SM (2005) Experience-driven plasticity of visual cortex limited by myelin and Nogo receptor. *Science* 309:2222–2226.
34. Dindot SV, Antalffy BA, Bhattacharjee MB, Beaudet AL (2008) The Angelman syndrome ubiquitin ligase localizes to the synapse and nucleus, and maternal deficiency results in abnormal dendritic spine morphology. *Hum Mol Genet* 17:111–118.
35. Yamasaki K, et al. (2003) Neurons but not glial cells show reciprocal imprinting of sense and antisense transcripts of *Ube3a*. *Hum Mol Genet* 12:837–847.
36. Niell CM, Stryker MP (2008) Highly selective receptive fields in mouse visual cortex. *J Neurosci* 28:7520–7536.